Limit of validity of Ostwald's rule of stages in a statistical mechanical model of crystallization

Lester O. Hedges and Stephen Whitelam*
Molecular Foundry, Lawrence Berkeley National Laboratory, 1 Cyclotron Road, Berkeley, CA 94720, USA

Molecular-resolution imaging reveals crystallization pathways of complex materials in which the parent phase first transforms into an intermediate phase before the stable phase emerges. We have only rules of thumb to predict when transient intermediates should appear prior to crystallization, chief among which is Ostwald's rule of stages. This rule states that the first phase to appear upon transformation of the parent phase is the one closest in free energy to it. Although often upheld, the rule is without theoretical foundation and is not universally obeyed. Lacking predictive general rules, one way of trying to understand material crystallization pathways is to consider simple models that capture important microscopic features of real systems, and to identify how these features govern the emergence or absence of crystallization precursors. Here we do so within a statistical mechanical model of anisotropic nanoparticle crystallization. We show how the thermodynamic landscape for crystallization is shaped by interparticle interactions, and how the crystallization pathway of the model is dictated both by this landscape and by the relative rate of particle rotations and translations. The range of behaviors seen is richer than can be predicted by Ostwald's rule, but it can be anticipated using simple microscopic theory.

Crystallization is of central importance to materials science, underpinning fields as diverse as metallurgy [1], drug synthesis [2] and protein characterization [3]. Our understanding of crystallization is considerable [4–6] but incomplete: we cannot predict precise rates of crystallization even in simple systems [7], and we cannot predict even *qualitative* pathways of crystallization in complex systems [8, 9]. Experiments call out for such understanding. Molecular-resolution imaging reveals crystallization pathways of complex materials – metal phosphates [10], proteins [11] and colloids [12], for instance – in which the parent phase first transforms into a transient intermediate phase before the stable solid phase emerges. Such pathways challenge the conventional picture of nucleation and growth, which assumes the formation of ordered structures from nuclei of similar order [13]. Indeed, excepting systems of simple isotropic particles [14–16], we have no theoretical framework for predicting a material's crystallization pathway.

We do possess important rules of thumb that suggest how a material *might* crystallize. Ostwald's rule of stages states that the parent phase will first transform into the metastable phase closest to it in free energy [17, 18]. The closely-related conjecture of Stranski and Totomanow [19] is the statement that the phase that first emerges is the one separated from the parent phase by the smallest free energy barrier. Both rules receive broad support. With respect to Ostwald's rule, sulfur crystallizes from solution via a dense liquid [17], while melts [20] and aerosols [21] also display precursors of the stable crystal. On the computer, a microscopic analog of the rule is seen: the freezing of polar fluids, model proteins [4] and molecular nitrogen [22] can all take place via critical nuclei whose composition differs markedly from that of the stable phase.

But Ostwald's rule is also observed to break down. Amino acid crystallization [23], the simulated freezing of molecular CO_2 [24], and Potts model phase transformations [25] can all take place without involvement of metastable polymorphs. Transient phases are seen prior to crystallization of the drug D-mannitol [26] and simulated Lennard-Jones particles [4, 27] at large supersaturation and small supercooling, respectively, but not under the converse conditions. Simulations of charged colloids show that sluggish dynamics can also invalidate the Stranski-Totomanow conjecture [28].

These rules, then, are limited. Ostwald's rule has no theoretical foundation [29], and is perhaps more useful as a classification scheme than for its predictive power. In the absence of effective general rules, one possible strategy for predicting experimental self-assembly pathways is to devise models designed to represent particular classes of materials, and to identify the microscopic controls of assembly pathways in these models. Here we adopt this approach and study a model designed to represent an important class of materials (such as proteins [6, 11] and patchy nanoparticles [30]) that form ordered phases stabilized by specific attractions and disordered phases stabilized by nonspecific attractions. We will describe how particle interactions shape the free energy landscape for crystallization, so favoring or disfavoring visitation of intermediate phases, and how the relative rate of particle translations and rotations can prove a decisive factor in this regard. The behavior seen in our simulations exceeds the scope of Ostwald's rule, but can be anticipated using simple microscopic theory.

Model and simulation details. We consider a collection of particles that live on a featureless two-dimensional

*swhitelam@lbl.gov

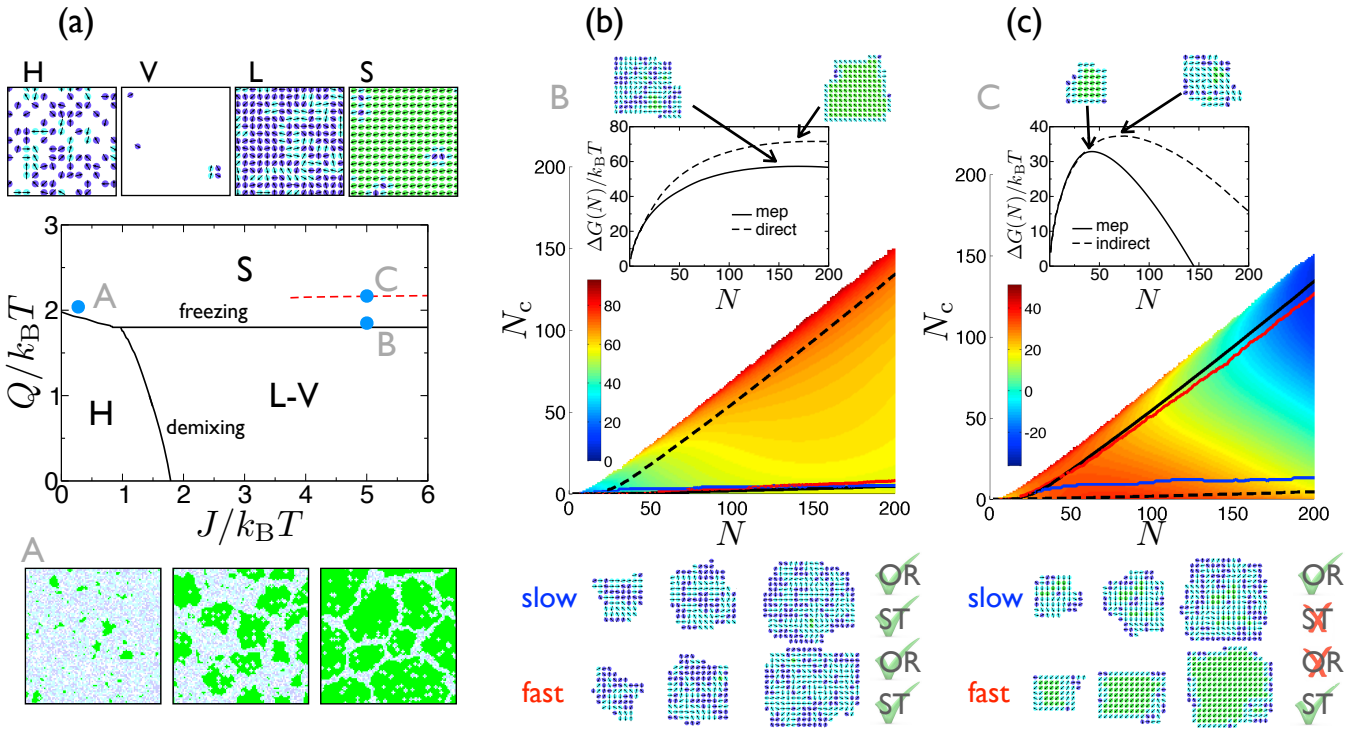

FIG. 1: (a) Model phase diagram with phase snapshots (top) and a dynamical trajectory from phase point A (bottom). At A, only phases H and S are viable, and the dynamics is straightforward: the solid emerges directly from the fluid. We focus instead on the regime of solid stability to the right of the demixing line, where the liquid lies between the metastable vapor and the stable solid in free energy. We show free energy surfaces in a space of cluster size N and crystallinity N_c, and dynamical trajectories for crystallization at points B (b) and C (c) in phase space. Solid black lines indicate the minimum energy path (mep) across the free energy suface; the black dashed line shows an energetically unfavorable pathway. The red and blue lines overlaid on the free energy surfaces represent the mean of ∼1000 independent dynamical trajectories for fast ($r = 99$) and slow ($r = 0.01$) rotations, respectively (Figs. S1–3). At point B the liquid becomes post-critical regardless of dynamic factors, satisfying Ostwald's rule (OR) in a microscopic (fast) or macroscopic (slow) sense. At C, direct or indirect trajectories can be followed, and the indirect one goes against the sense of the Stranski-Totomanow (ST) conjecture. Thermodynamics favors a critical nucleus with a liquidlike composition below the dashed red line on the phase diagram. Even above this line, though, sluggish kinetics can lead to the emergence of a relic of the liquid phase.

substrate, which we model as a square lattice of N sites. Sites may be vacant or be occupied by a particle. Nearest-neighbor particles receive an interaction energy reward of $-J$ (a nonspecific mode of binding). Particles are anisotropic, and may point in any of R discrete directions. Neighboring particles receive an additional energetic reward of $-Q$ if they are aligned (a specific mode of binding), and a penalty of $+Q$ if they are antialigned (in terms of experimental controls, some proteins' specific attractions can be modulated by altering the concentration of divalent cations, and nonspecific depletion attractions can be induced by adding inert objects to solution). R is related to an angular specificity: the larger is R, the more precisely two particles must align before they receive the specific binding reward. Each particle on the substrate feels a chemical potential $-\mu$. The resulting model is similar to those of Refs. [31, 32], and we follow the authors of the latter work in choosing $R = 24$ as a concrete choice on which to focus. We will also discuss the important effects seen on varying R.

We simulated our model using the grand canonical Metropolis Monte Carlo procedure described in Supporting Information 1 (SI1). This procedure allows particles to translate (adsorb to and desorb from the substrate), and to rotate in place on the substrate. We have explored the effect of varying extensively the relative proposal rate r of rotations and translations, because we are interested in how particles of different sizes crystallize. Stokes' law predicts the relative rate of rotation and translation of a particle of girth a to scale as a^{-2}, and one would therefore expect a change of this basic rate by four orders of magnitude upon moving from a protein of $a \sim 1$ nm to a patchy nanoparticle of $a \sim 100$ nm. The limit of sluggish rotations might also be appropriate for materials like DNA-linked colloids that experience little rotational freedom when bound [33]. We used this simulation protocol to calculate the model's phase diagram; we used it in concert with umbrella sampling [4, 34] to calculate free

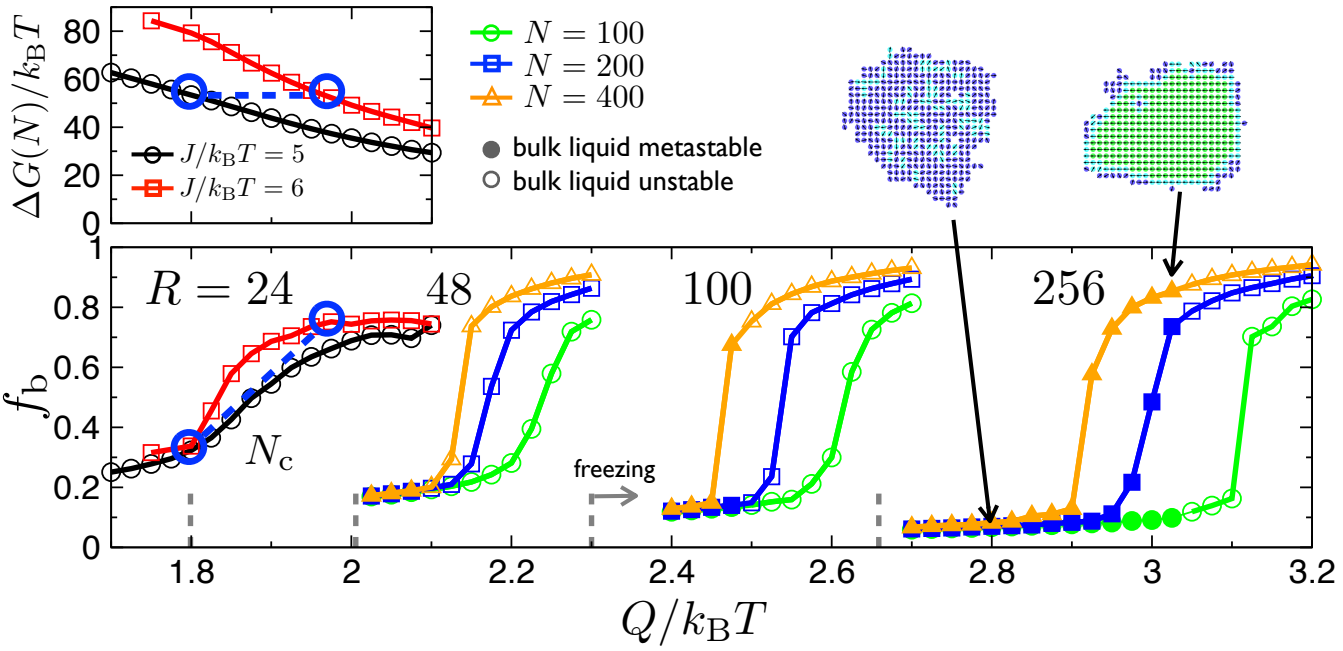

FIG. 2: When three phases (V, L, C) are viable, the thermodynamically-favored crystallization pathway is determined by the potency Q and angular specificity R of specific binding. Main panel: fraction of crystalline bonds f_b (number of pairwise contacts between aligned particles, divided by total number of pairwise contacts) in nuclei (critical, labeled N_c, or of specified size, labeled by that size), calculated from umbrella sampling simulations for four values of R (24, 48, 100 and 256; we set $J = 5\,k_BT$ ($R = 48$), $J = 4\,k_BT$ ($R = 100$), and $J = 3\,k_BT$ ($R = 256$), to keep the size of the critical nucleus manageable). The positions of the freezing line for each value of R are shown by vertical gray dashed lines. Solid (open) symbols indicate that the bulk liquid is metastable (unstable) to crystallization. In general, nuclei are liquidlike near the freezing line, and become crystalline as Q is increased. How much of the liquid is seen depends strongly upon where one lies in parameter space (and upon dynamics), and is not revealed by appealing to Ostwald's rule. Top panel: free energy barriers to nucleation for $R = 24$ at two values of J. As shown by the blue circles, one can identify regions of phase space in which nucleation barriers are similar, but the character of critical nuclei are qualitatively different.

energy surfaces in a space of nucleus size and degree of crystallinity; and we used it in concert with transition path sampling [35, 36] and forward flux sampling [37] to generate a statistically significant number of unbiased dynamical trajectories. This set of methods reveals the distinct effect on crystallization of thermodynamic and dynamic factors.

Results. In Fig. 1 (a) we show the phase diagram of the model in a space of the strength of the nonspecific mode of binding J and the specific mode of binding Q. Snapshots of phases are given in the top panel: particles with 4 parallel neighbors (crystalline particles) are shown green; particles with no parallel neighbors (fluid particles) are dark blue. When both interactions are weak the stable phase is a homogeneous fluid phase (H) of moderate density. When Q is large enough (above the 'freezing line'), the solid (S) is stable. At point A in phase space, only phases H and S are viable, and crystallization consists of the direct transformation of H into S (Fig. 1(a)). When J is sufficiently large (to the right of the 'demixing line'), phase H disappears and dense liquid (L) and sparse vapor (V) phases become viable (in off-lattice analogs of our model we would also expect dense solid phases to become viable at large values of J [38]). Our choice of μ (see SI) ensures that to a mean-field approximation liquid and vapor phases are equal in free energy. In simulations, orientational correlations in the liquid lower its free energy below that of the vapor. As a consequence, above the freezing line and to the right of the demixing line the liquid phase lies intermediate in free energy between the vapor phase and the stable solid. Starting from an empty substrate, does the liquid emerge prior to crystallization?

We first focus on point B on the phase diagram. Here an empty substrate immediately becomes host to the metastable low-density vapor (the larger is J, the more strongly metastable is the vapor: in a mean-field approximation, J controls the depth of the Ising model 'double well' (see SI2)). We show in Fig. 1(b) the free energy of formation from the vapor of a nucleus as a function of its size N and the number of crystalline particles N_c it contains. The minimum energy pathway (solid line) from the vapor to the crystal is an indirect one that displays a liquidlike critical nucleus. The direct pathway (dashed line) via a crystalline critical nucleus is disfavored by about 20 k_BT. The indirect pathway is made possible by the intermediate liquid phase, but because we are far from the

demixing line is not a result of critical liquid-vapor density fluctuations [14]. Dynamical trajectories (red and blue lines, $r = 99$ and 0.01, respectively) adhere to the indirect pathway, regardless of the relative rate of particle rotations and translations. A liquid nucleates on the substrate, and only subsequently does the crystal emerge from the liquid. For rapid rates of rotation the postcritical liquid readily transforms into a crystal while still only of small size (Fig. S1, right panel); for the small value of R considered here there are no appreciable barriers to nucleation of the crystal in the bulk liquid. However, for sluggish rotation rates (Fig. S1, left panel), the liquid consumes the substrate, and fails to crystallize during the course of the simulation.

We next move to point C in phase space, increasing the strength Q of the specific mode of binding. The liquid remains intermediate in free energy between the parent phase and the stable solid, but the driving force for crystallization has changed qualitatively: the *direct* pathway, with a crystalline critical nucleus, is preferred! The indirect pathway with a liquidlike critical nucleus is still viable, but is disfavored by about $5\,k_{\mathrm{B}}T$. Because of this relatively small discrepancy in barrier heights, both pathways can be seen in dynamic simulations. For a sufficiently rapid rotation rate (red line, $r = 99$) the direct pathway is taken: a crystal nucleates and grows on the substrate. No liquid is seen. For sluggish rotation rates (blue line, $r = 0.01$), by contrast, the indirect pathway *is* seen, and the substrate is again consumed by a liquid (see Fig. S2 and S3).

We therefore see that a relic of the liquid phase can influence the crystallization pathway some way past the freezing line, but that eventually thermodynamics favors a direct mode of crystallization: the critical nucleus is crystalline above the horizontal red line on the phase diagram. The question of how much liquid is seen in simulations is one that cannot be addressed by Ostwald's rule. Assuming that it can be applied (it pertains to metastable intermediate phases, and the liquid at B and C is at most weakly so), it is satisfied in a macroscopic sense by the 'slow' trajectories at point B (because here a liquid consumes the substrate), but only in a microscopic sense by the 'fast' trajectories (because the postcritical liquid blob crystallizes before it grows appreciably). It is violated by the 'fast' trajectories at C, but not by the 'slow' trajectories. Moreover, the latter trajectories involve passage over a free energy barrier larger than the smallest available, going against the sense of the Stranski-Totomanow conjecture.

The microscopic control of the thermodynamically-preferred crystallization mechanism is (for J near or past the demixing line) the competition between the angular specificity R and potency Q of specific binding, which shapes the free energy landscape for crystallization so as to encourage or discourage appearance of a relic of the liquid phase. In Fig. 2 we show that the composition of the critical nucleus (and of nuclei of fixed sizes) changes from being liquidlike to being crystalline as one moves vertically away from the freezing line on the phase diagram. This trend holds for a range of values of R, a parameter that describes in a coarse way the angular specificity of the directional attraction (note that the the larger is R, in general, the more strongly is the liquid metastable with respect to crystallization; see Fig. S4–5). The results of Fig. 2 show a range of behaviors: depending on where one lies in phase space, the smallest crystalline cluster preferred by thermodynamics is sometimes pre-critical, and sometimes post-critical. Sometimes a liquid dominates the crystallization pathway even when its bulk counterpart is unstable (small R, small Q); sometimes a crystallite can be lower in free energy than a small liquid blob whose bulk counterpart is metastable (large R, large Q). How much liquid is seen in a simulation depends on this thermodynamic preference, but also upon the relative rate of particle rotations and translations.

We note also that changes of temperature [32] and supersaturation can change crystallization mechanism, but that neither is its direct control. In Fig. 2 (top panel) we show that there is no simple correlation between the height of the free energy barrier to nucleation and the nature of the crystallization pathway (materials reported in the introduction, for instance, also show no clear trend in this regard, and, indeed, Ostwald's rule pertains to either a metastable or an unstable parent phase). Lines of varying temperature on the phase diagram of Fig. 1 are for fixed J and Q straight ones that pass through its origin: changing T can indeed change crystallization mechanism, but sometimes in a complicated and indirect way (see Fig S6).

Clearly, rules of thumb are of limited use here. But, interestingly, we can anticipate using simple *microscopic* theory the manner in which the model's parameters dictate its preferred crystallization pathway. We calculated the model's bulk free energy analytically, in a self-consistent mean-field approximation, as a function of order parameters ρ (density) and τ (crystallinity). This free energy is given in SI2. From this we obtained the phase diagram shown in Fig. 3, which resembles qualitatively its simulated counterpart. Bulk free energy surfaces do not properly represent surface tensions between phases, and so cannot be a decisive measure of the preferred pathway for crystallization. However, they are strongly suggestive of that pathway, being the principal driving force for crystallization, and have been used to infer, for example, crystallization pathways of isotropic particles [15, 16]. Here, by calculating on bulk surfaces the preferred pathway between parent and solid phases, we can shade the phase diagram according to how 'direct' is this pathway, and so visualize the change of thermodynamic crystallization mechanism engineered by changes of microscopic parameters (Fig. 3 and Figs. S4–7). Although the locations of these changes of mechanism are not in quantitative

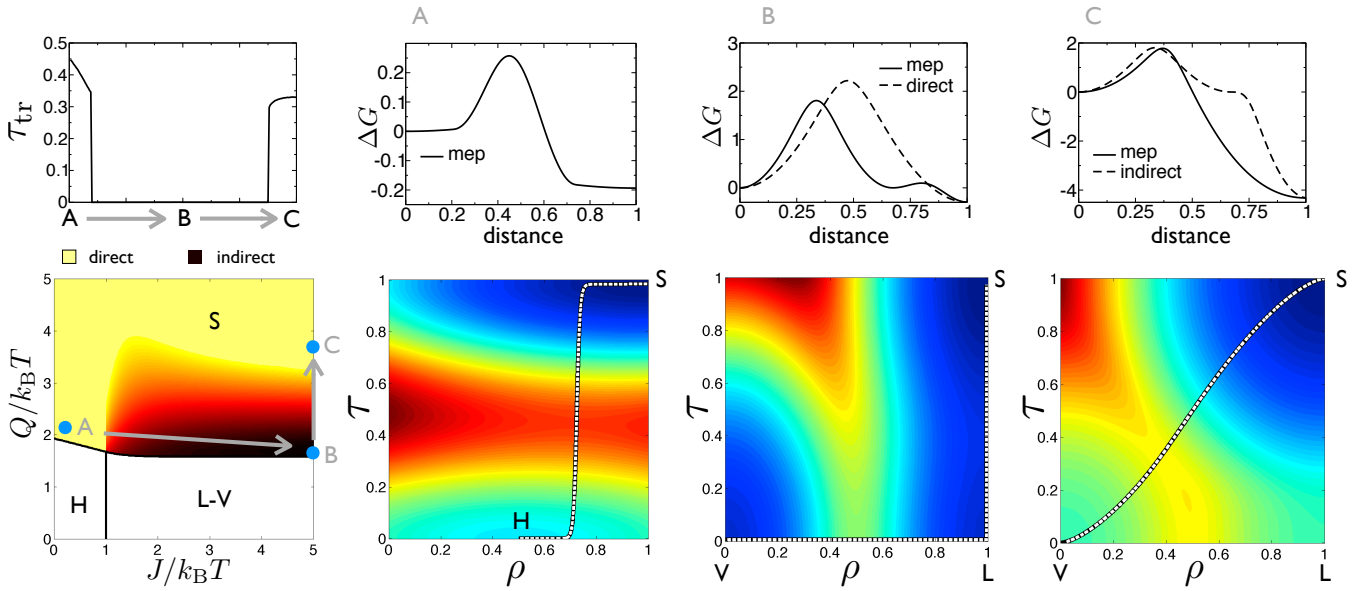

FIG. 3: Visualizing the shaping of crystallization landscapes by microscopic parameters. Mean-field phase diagram (bottom left) and free energy surfaces at points A, B, and C (left to right) in phase space. Dashed white lines show the minimum energy path (mep) on each surface, calculated using the string method [39]. Above each surface we show free energy along this path (solid line, compared to a direct path at B and an indirect path at C). On moving across the phase diagram from A $\rightarrow$ B $\rightarrow$ C we observe qualitative changes of the character of the bulk driving force, from direct (with no intermediate phases favored) to indirect (vapor-to-liquid-to-solid) and back again. These trends are qualitatively consistent with those seen in our computer simulations. We summarize the crystallization mechanism by shading the phase diagram according to where direct (light) and indirect pathways (dark) are favored. Above it, we plot the degree of crystallinity τ_{tr} at the transition state as a function of phase space location (we move in a line from A to B, and then from B to C; see also Fig. S4). A large value of τ_{tr} shows the transition state to be crystalline, and the preferred path to be direct.

accord with our simulations, the trends observed mirror those findings qualitatively: indirect crystallization pathways become viable to the right of the demixing line, and are supplanted by a direct mechanism some distance above the freezing line. The location of this crossover and of the limit of liquid metastability also change with R (Fig. S7) in a manner similar to that seen in our simulations (Fig. 2).

We have identified the microscopic controls of crystallization in a model of anisotropic particles that may associate in a nonspecific and a specific way, designed to mimic patchy nanoparticles or proteins. Our model addresses orientational order and does not allow positional order [40]; it would be interesting to explore the effect of coupling both. We have also focused on the influence on crystallization of relics of bulk phases, although mesoscale structures without counterparts on the bulk phase diagram can also profoundly influence crystallization pathways [41, 42]. The effect of our model's microscopic parameters on the thermodynamic landscape for crystallization can be anticipated in a qualitative way using mean-field theory, an observation that adds to evidence suggesting that microscopic calculations can be used to predict material assembly pathways [15, 16]. To this approximation we summarize in Figs. 3 and S7 our expectation for the thermodynamically preferred crystallization pathway of our model as a function of its microscopic parameters J, Q and R. The nature of the pathways we have observed in simulations depend on both thermodynamic and dynamic factors. In general, we expect the propensity for indirect pathways to crystallization to be large for particles with highly specific anisotropic interactions and for slowly-rotating particles (e.g. large particles or particles that experience little rotational freedom when bound). Some of the behavior we have seen can be explained by appealing to Ostwald's rule, and some of it cannot. Nonetheless, Ostwald's rule provides a framework for classifying material assembly pathways, and its limitations should motivate us to look for microscopically-grounded rules to replace it.

Acknowledgements. We thank Daan Frenkel, Phill Geissler, Lutz Maibaum and Will McKerrow for discussions, and Jim De Yoreo, Rob Jack and Daphne Klotsa for valuable comments on the manuscript. L.O.H. was supported by the Center for Nanoscale Control of Geologic CO_2, a U.S. D.O.E. Energy Frontier Research Center, under Contract No. DE-AC02–05CH11231. This work was done at the Molecular Foundry, Lawrence Berkeley National Laboratory, and was supported by the Director, Office of Science, Office of Basic Energy Sci-

ences, of the U.S. Department of Energy under Contract No. DE-AC02–05CH11231.

[1] R. DeHoff, *McGraw-Hill Series in Materials Science and Engineering: Thermodynamics in Materials Science* (McGraw-Hill, Boston, Massachusetts, 1993).

[2] J. C. Burley, M. J. Duer, R. S. Stein, and R. M. Vrcelj, European Journal of Pharmaceutical Sciences **31**, 271 (2007), ISSN 0928-0987.

[3] L. Slabinski, L. Jaroszewski, A. P. C. Rodrigues, L. Rychlewski, I. A. Wilson, S. A. Lesley, and A. Godzik, Protein Science **16**, 2472 (2007).

[4] P. R. Wolde and D. Frenkel, Physical Chemistry Chemical Physics **1**, 2191 (1999).

[5] R. P. Sear, Journal of Physics: Condensed Matter **19**, 033101 (2007).

[6] O. Galkin and P. G. Vekilov, Proc. Nat. Acad. Sci. **97**, 6277 (2000).

[7] S. Auer and D. Frenkel, Nature **409**, 1020 (2001), ISSN 0028-0836.

[8] D. Mangin, F. Puel, and S. Veesler, Organic Process Research & Development **13**, 1241 (2009), ISSN 1083-6160.

[9] M. Niederberger and H. Cölfen, Physical Chemistry Chemical Physics **8**, 3271 (2006).

[10] S. Y. Chung, Y. M. Kim, J. G. Kim, and Y. J. Kim, Nature Physics **5**, 68 (2008), ISSN 1745-2473.

[11] S. Chung, S. H. Shin, C. R. Bertozzi, and J. J. De Yoreo, Proceedings of the National Academy of Sciences (2010).

[12] T. H. Zhang and X. Y. Liu, Angew. Chem. Int. Ed **48**, 1308 (2009).

[13] D. Erdemir, A. Y. Lee, and A. S. Myerson, Accounts of Chemical Research pp. 801–808 (2009).

[14] P. R. Wolde and D. Frenkel, Science **277**, 1975 (1997).

[15] Y. C. Shen and D. W. Oxtoby, Physical Review Letters **77**, 3585 (1996).

[16] J. Lutsko and G. Nicolis, Physical Review Letters **96**, 046102 (2006).

[17] W. Ostwald, Z. Phys. Chem. **22** (1897).

[18] T. Threlfall, Organic Process Research & Development **7**, 1017 (2003), ISSN 1083-6160.

[19] I. N. Stranski and D. Totomanov, Z. Phys. Chem **163**, 399 (1933).

[20] R. E. Cech, Transactions of the American Institute of Mining, Metallurgical, and Petroleum Engineers, Incorporated p. 585 (1957).

[21] L. E. Fox, S. C. Wofsy, D. R. Worsnop, and M. S. Zahniser, Science **267**, 351 (1995).

[22] J. M. Leyssale, J. Delhommelle, and C. Millot, Chemical Physics Letters **375**, 612 (2003).

[23] M. Kitamura, CrystEngComm **11**, 949 (2009).

[24] J. M. Leyssale, J. Delhommelle, and C. Millot, The Journal of Chemical Physics **122**, 184518 (2005).

[25] D. Sanders, H. Larralde, and F. Leyvraz, Physical Review B **75**, 132101 (2007), ISSN 1550-235X.

[26] J. Cornel, P. Kidambi, and M. Mazzotti, Industrial & Engineering Chemistry Research **49**, 5854 (2010).

[27] W. C. Swope and H. C. Andersen, Physical Review B **41**, 7042 (1990), ISSN 1550-235X.

[28] E. Sanz, C. Valeriani, D. Frenkel, and M. Dijkstra, Physical Review Letters **99**, 55501 (2007).

[29] P. Cardew, R. Davey, and A. Ruddick, Journal of the Chemical Society, Faraday Transactions 2 **80**, 659 (1984).

[30] S. C. Glotzer and M. J. Solomon, Nature materials **6**, 557 (2007), ISSN 1476-1122.

[31] S. Whitelam, J. Chem. Phys. **132**, 194901 (2010).

[32] N. Duff and B. Peters, The Journal of Chemical Physics **131**, 184101 (2009).

[33] W. Dai, S. K. Kumar, and F. W. Starr, Soft Matter (2010).

[34] G. Torrie and J. Valleau, Journal of Computational Physics **23**, 187 (1977).

[35] P. G. Bolhuis, D. Chandler, C. Dellago, and P. L. Geissler, Annual Review of Physical Chemistry **53**, 291 (2002).

[36] A. Pan and D. Chandler, J. Phys. Chem. B **108**, 19681 (2004).

[37] R. Allen, P. Warren, and P. Ten Wolde, Physical Review Letters **94**, 18104 (2005), ISSN 1079-7114.

[38] S. Whitelam, Physical Review Letters **105**, 88102 (2010), ISSN 1079-7114.

[39] E. Weinan, W. Ren, and E. Vanden-Eijnden, J. Chem. Phys. **126**, 164103 (2007).

[40] J. Doye, A. Louis, I. Lin, L. Allen, E. Noya, A. Wilber, H. Kok, and R. Lyus, Physical Chemistry Chemical Physics **9**, 2197 (2007), ISSN 1463-9076.

[41] O. Henrich, K. Stratford, D. Marenduzzo, and M. E. Cates, Proc. Natl. Acad. Sci. USA **107**, 13212 (2010).

[42] J. W. P. Schmelzer, J. Schmelzer Jr, and I. S. Gutzow, The Journal of Chemical Physics **112**, 3820 (2000).